JOURNAL OF COMPUTATIONAL PHYSICS 40, 376–395 (1981)

High Order Accurate, Explicit, Difference Formulas for the Classical Wave Equation*

CHI-HUA HUANG AND JOHN H. CUSHMAN†

Purdue University, West Lafayette, Indiana 47907

Received December 21, 1979; revised July 8, 1980

This article presents a simple and yet very novel approach to developing difference schemes for wave equations. The schemes that are developed are explicit in nature. The schemes are of such generality that one can transform from one difference scheme to another with only the slightest of computational effort. The schemes exhibit dispersive errors. The errors can be minimized, however, by increasing the order of truncation error. Numerical results are presented for two linear model equations with truncation error ranging up to $O(h^5)$. Numerical results are also presented for a system of shallow water equations. By choosing the appropriate α for a first order linear equation (α defines the geometry of an element) we may generate stable schemes for an arbitrary Courant number.

1. INTRODUCTION

Generally, the solution to a wave equation at a point in time–space is only a function of a limited amount of data. Consider the following two canonical examples:

$$\text{(i)} \qquad u_t + cu_x = 0,\ u(x, 0) = f(x) \tag{1.1}$$

and

$$\text{(ii)} \qquad u_{tt} - c^2 u_{xx} = 0,\ u(x, 0) = f(x),\ u_t(x, 0) = g(x). \tag{1.2}$$

The solutions to (1.1) and (1.2) are, respectively,

$$u(x, t) = f(x - ct) \tag{1.3}$$

and

$$u(x, t) = \tfrac{1}{2}[f(x - ct) + f(x + ct)] + \frac{1}{2c}\int_{x-ct}^{x+ct} g(\tau)\, d\tau \tag{1.4}$$

(see, e.g., Weinberger [10]). Clearly the solution of (1.1) is propagated along the characteristic curve $\chi = x - ct$. Similarly the solution of (1.2) at a point (x, t) is only

* Contribution from the Purdue Agric. Exp. Stn., West Lafayette, Ind. 47907. Journal Paper No. 7939.

† Graduate Assistant and Assistant Professor of Soil Physics, respectively, Purdue University.

0021-9991/81/040376-20$02.00/0

a function of the triangular data set lying between the characteristics $\chi = x - ct$ and $\eta = x + ct$.

It is the limited data sets associated with wave equations that lead to our efficient and accurate schemes. A good numerical scheme should take full advantage of a wave equation's limited data set, e.g., Stroud [8].

Many finite difference equations are available for solving the various wave equations (see, e.g., Roache [6]). Generally, higher order accurate wave equation solvers are multi-step schemes (see, e.g., the third order accurate schemes of Rusanov [7], and Warming *et al.* [9]). A well-known single-step, explicit, second order accurate scheme is the Lax–Wendroff method (see, e.g., Roache [6, p. 357]). All the schemes that we will construct will be single-step explicit, however, the order of accuracy will be variable.

In this article we will use a modified space–time finite element technique for deriving difference equations. Several preliminary results using the method were presented in Cushman [1, 2].

2. Numerical Technique

As partially outlined in Cushman [1], we will employ a modified Galerkin technique in space–time. Figure 2.1 illustrates the region over which we will apply Galerkin's method. The novelty here is that rather than use all of space–time or even a rectangular strip of space–time (Fig. 2.2), we are using only a very small subset of a single space–time strip in our analysis. This of course (as outlined in the introduction) is perfectly justifiable for the wave equations under consideration.

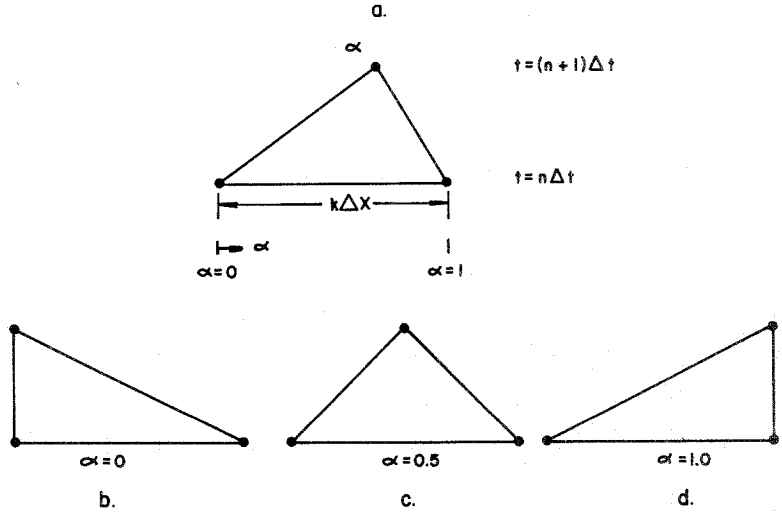

FIG. 2.1. Triangular elements—the shape is governed by the parameter α. k is the order of polynomial interpolation. (a) arbitrary α, (b) $\alpha = 0$, (c) $\alpha = 0.5$, (d) $= 1.0$.

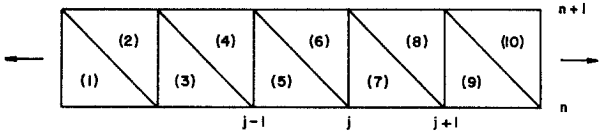

FIG. 2.2. Standard discretization of a portion of space–time not used in this article.

By merely varying the order of the polynomial interpolation and the shape of the element we may create numerous difference schemes of arbitrary high order accuracy.

The Galerkin equation for (1.1) is given by

$$0 = \int_{\Omega_e} \Phi_i \left[\frac{\partial \Phi_j}{\partial t} + c \frac{\partial \Phi_j}{\partial x} \right] d\Omega \, u_j, \tag{2.1}$$

where Φ_i represents a global (local) interpolating polynomial and test function; u_j is the known (unknown) value of u at node j; Ω_e is the area of the space–time triangular element; the indices i and j run from one to the number of nodes in the element (throughout this article barycentric coordinates will be used); and repeated indices imply summation.

Consider for example linear Lagrange interpolating polynomials coupled with Galerkin's minimization method applied to (1.1). It was shown in Cushman [2] for $\alpha = 0.0$, 0.5, and 1.0, respectively (see Fig. 2.1), that the resulting difference schemes are: (i) unstable Euler, (ii) first order accurate Lax method which is stable for $\nu \leqslant 1$, and (iii) a first order accurate upstream differencing method which also is stable for $\nu \leqslant 1$. The Courant number ν is of course $c\,\Delta t/\Delta x$.

If $\alpha = 0.5$ in Fig. 2.1 and quadratic Lagrange interpolation is used with Galerkin's method applied to (1.1), the resulting difference scheme is (Cushman [2]) the single-step, $O(\Delta t^2, \Delta x^2)$, Lax–Wendroff method which again is stable for $\nu \leqslant 1$. For clarification, the linear and quadratic equations for arbitrary α are given in the Appendix.

We can apply the method of single space–time elements to (1.2). Instead, however, we choose to apply it to an equivalent system. In particular, u and v of the system

$$\begin{aligned} u_t + cv_x &= 0, \qquad u(x,0) = f(x), \\ v_t + cu_x &= 0, \qquad v(x,0) = g(x), \end{aligned} \tag{2.2a}$$

will satisfy the second order equation (1.2). In fact any second order one-dimensional equation can be decomposed into a system of first order equations.

The Galerkin equation for (2.2a) with the notation of (2.1) is given by

$$\begin{aligned} 0 &= \int_{\Omega_e} \Phi_i \frac{\partial \Phi_j}{\partial t} d\Omega \, u_j + c \int_{\Omega_e} \Phi_i \frac{\partial \Phi_j}{\partial x} d\Omega \, v_j, \\ 0 &= \int_{\Omega_e} \Phi_i \frac{\partial \Phi_j}{\partial t} d\Omega \, v_j + c \int_{\Omega_e} \Phi_i \frac{\partial \Phi_j}{\partial x} d\Omega \, u_j. \end{aligned} \tag{2.2b}$$

If l is the number of unknown nodal values of u and m is the number of known nodal values in the element (Fig. 2.1), the general form of (2.1) in matrix notation can be written as

$$\left(\begin{array}{c|c} C & \\ \hline -B & A \end{array}\right)\begin{pmatrix} \bar{y} \\ \bar{x} \end{pmatrix} = \bar{0}, \tag{2.3a}$$

where C has dimension $m \times (l+m)$, B has dimension $l \times m$, A has dimension $l \times l$, $\bar{y}$ is the vector of known nodal values, and $\bar{x}$ is the vector of unknown nodal values.

Thus

$$C\begin{pmatrix} \bar{y} \\ \bar{x} \end{pmatrix} = \bar{0} \tag{2.3b}$$

corresponds to the equations for the nodes with known nodal values of u and

$$(-B \mid A)\begin{pmatrix} \bar{y} \\ \bar{x} \end{pmatrix} = \bar{0} \tag{2.3c}$$

corresponds to the equations for the nodes with unknown nodal values of u.

Hence, we need only examine the system

$$\bar{x} = A^{-1}B\bar{y}. \tag{2.3d}$$

The matrix equation associated with (2.2b) may be developed in the same fashion, only in the case of (2.2b) there are two unknowns and hence two equations for each node.

Of course (2.3d) contains much more information than necessary. The entirety of information we need is given by the row of $A^{-1}B$ which corresponds to the location in the vector $\bar{x}$ with the value of u at the $(n+1)$st time level. For example, if quadratic interpolation is used with (2.1) and $\alpha = 0.5$, the resulting equation corresponding to (2.3) has the form.

$$\begin{pmatrix} u_{j+1/2}^{n+1/2} \\ u_j^{n+1} \\ u_{j-1/2}^{u+1/2} \end{pmatrix} = \begin{pmatrix} a_{11} & a_{12} & a_{13} \\ a_{21} & a_{22} & a_{23} \\ a_{31} & a_{32} & a_{33} \end{pmatrix} \cdot \begin{pmatrix} u_{j-1}^n \\ u_j^n \\ u_{j+1}^n \end{pmatrix} \tag{2.4}$$

and hence,

$$u_j^{n+1} = a_{21}u_{j-1}^n + a_{22}u_j^n + a_{23}u_{j+1}^n, \tag{2.5}$$

i.e., we need only row two in $A^{-1}B$. Here, if the details are worked out (see Appendix) we find $a_{21} = (v/2)(1+v)$, $a_{22} = 1 - v^2$, and $a_{23} = (v/2)(v-1)$,

For polynomial interpolation higher than degree three it is impractical to invert A analytically. Thus we can not determine a closed form for the corresponding

difference scheme for u at the $(n+1)$st time level. All difference schemes of order greater than three are therefore determined in the machine.

3. Heuristic Stability and Truncation Analysis

It is well known (cf. Oden and Reddy [5]) that the Euclidian space interpolation error for kth degree interpolation polynomials over triangular elements has the form:

$$\operatorname*{Sup}_{\bar{x}\in\Omega_e} \|D^m(u(\bar{x})-\tilde{u}(\bar{x}))\| \leqslant c_{k+1}\frac{h^{k+1}}{d^m}, \tag{3.1}$$

where D^m is the mth Frechet derivative (cf. Wouk [11, p. 267]), h is the $\max\{h_e\}$, $h_e = \max_{\bar{x},\bar{y}\in\bar{\Omega}_e}|\bar{x}-\bar{y}|$, $d=\min_e\{d_e\}$, $d_e = \sup\{\text{diameter of all spheres contained in } \Omega_e\}$, $u(\bar{x})$ is the exact solution, and $\tilde{u}(\bar{x})$ is the polynomial approximation.

If we let the elements shrink in a regular fashion, R.H.S. (3.1) takes the form $c_{k+1}h^{k+1-m}$. Thus, since we are approximating the first derivative ($m=1$) in time and space of u for (1.1) we expect the order of accuracy of the corresponding difference scheme to be $O(h^k)$. And in fact, the analytical schemes for first ($k=1$) and second ($k=2$) order polynomials show this to be the case. Similarly, numerical tests show this result holds for higher order polynomials. For (1.2) the schemes are $O(h^{k-1})$, however, if (1.2) is decomposed into the system of first order equations (2.2a) the schemes are $O(h^k)$.

The stability of the difference schemes can also be very easily determined in a heuristic fashion. Consider first (1.1). The corresponding characteristic equation is $dt/dx = 1/c$ and the solution to (1.1) is (1.3). Clearly the solution to (1.1) is propagated along the characteristic equation. One is thus led to believe that stable schemes will result only when Galerkin's method is applied over a region containing the characteristic data. This in fact turns out to be the case for all orders of polynomials we have examined (up to order 5). Thus, for example, with quintic interpolation, if $v > 5\alpha$ or $v < 5(\alpha-1)$, the difference schemes associated with (2.1) are unconditionally unstable and if $5(\alpha-1)\leqslant v\leqslant 5\alpha$, they are conditionally stable, as will be illustrated in the numerical results section. We should also point out that for the linear and quadratic cases this heuristic stability can be verified analytically (see Cushman [2]).

A similar analysis applies to (1.2); only in this case the region over which Galerkin's method is applied must contain all of the data set illustrated in the introduction.

4. Computational Procedure and Numerical Results for Linear Equations

The computational procedure is quite simple. The only operation that consumes much time is the inversion of the matrix A in (2.3d). For a fixed v, A, however, need

TABLE I

Order of polynomial	Number of unknowns l	Number of knowns m
1. $O(h)$	1	2
2. $O(h^2)$	3	3
3. $O(h^3)$	6	4
4. $O(h^4)$	10	5
5. $O(h^5)$	15	6

Note. Dimension $A = l \times l$, dimension $B = l \times m$.

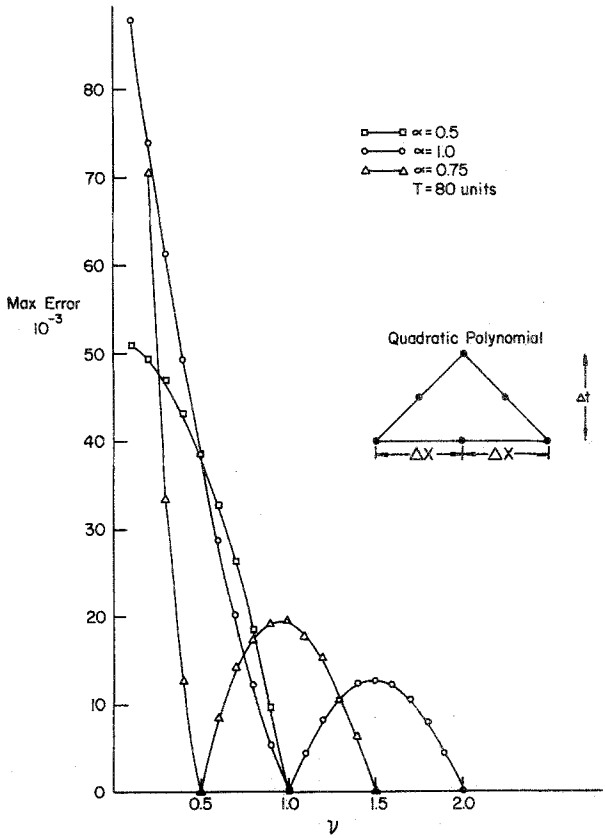

FIG. 4.1. Results for (1.1) with sine wave initial data with quadratic interpolation. When $\alpha = 0.5$ the difference scheme is the classical Lax–Wendroff. Note errors are $O(h^2)$.

be inverted only once. In the numerical results to be presented A^{-1} is accurate to 12 digits. When barycentric coordinates (Lagrange interpolating polynomials) are used, all components of A and B can be and were integrated analytically.

The dimensions of A and B for various order polynomial interpolants with (1.1) are in Table I. The dimensions are doubled for (2.2a). As an example consider the $O(h^5)$ scheme. In this case A is 15×15 and needs to be inverted (to 12-digit accuracy), but only the row of A^{-1} corresponding to u at the $(n+1)$st time level need be multiplied by the 15×6 matrix B.

Consider the following example:

$$u_t + cu_x = 0, \qquad u(x, 0) = \sin x, \tag{4.1}$$

the solution to which is $u(x, t) = \sin(x - ct)$. Figures 4.1 through 4.4 represent the error in the numerical results to the problem ranging from second order accurate to fifth order accurate. The figures represent plots of the maximum error vs the

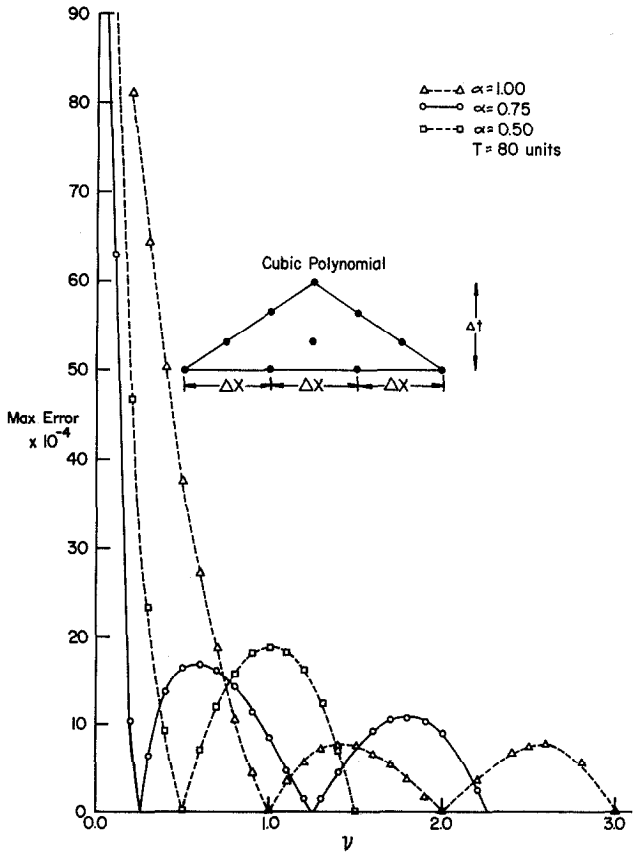

FIG. 4.2. Results for (1.1) with sine wave initial data with cubic interpolation.

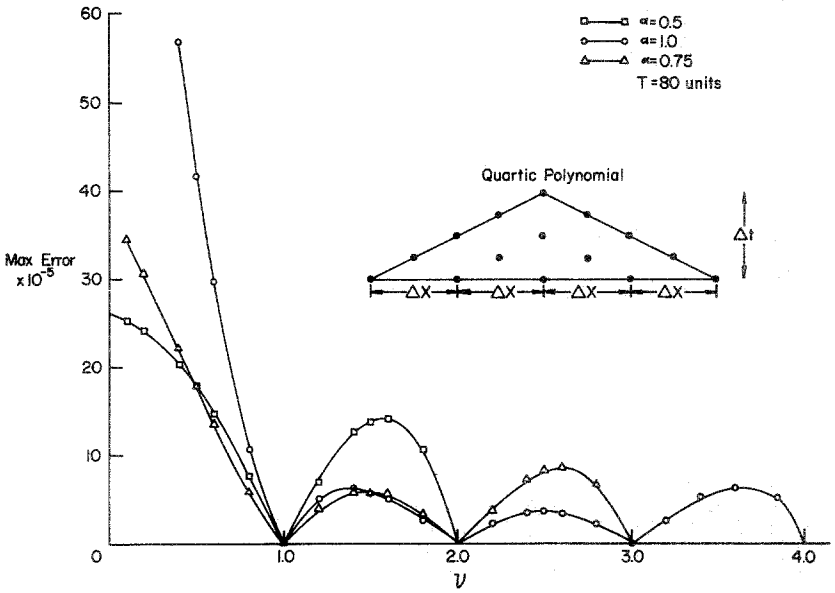

FIG. 4.3. Results for (1.1) with sine wave initial data with quartic interpolation. $O(h^4)$ error. Note also that the number of points where the exact solution is obtained has increased over Figs. 4.1 and 4.2.

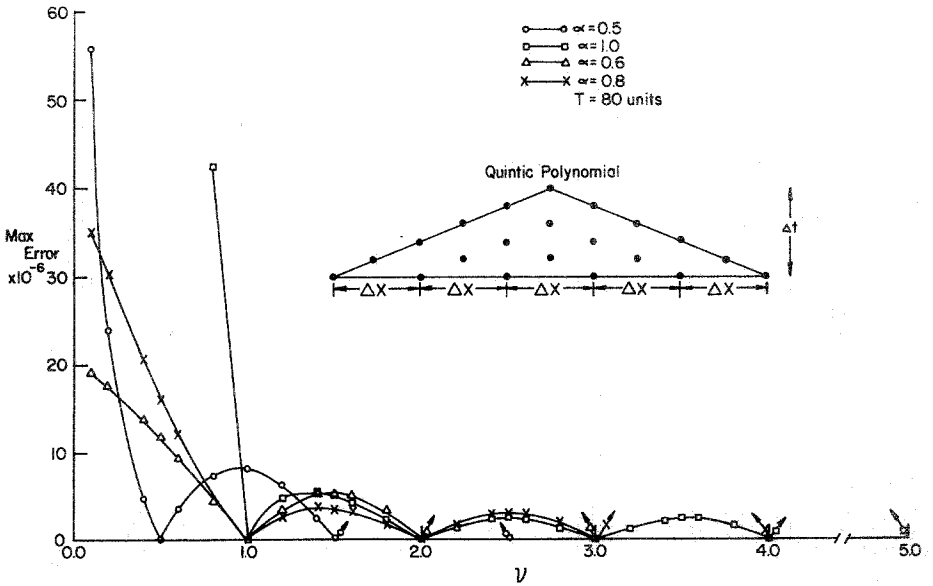

FIG. 4.4. Results for (1.1) with sine wave initial data with quintic interpolation. Errors are now of $O(h^5)$ with the exceptions of the regions between the arrows, e.g., ↗ ↖ indicates the region for $\alpha = 1.0$ within which the error is $O(h^3)$.

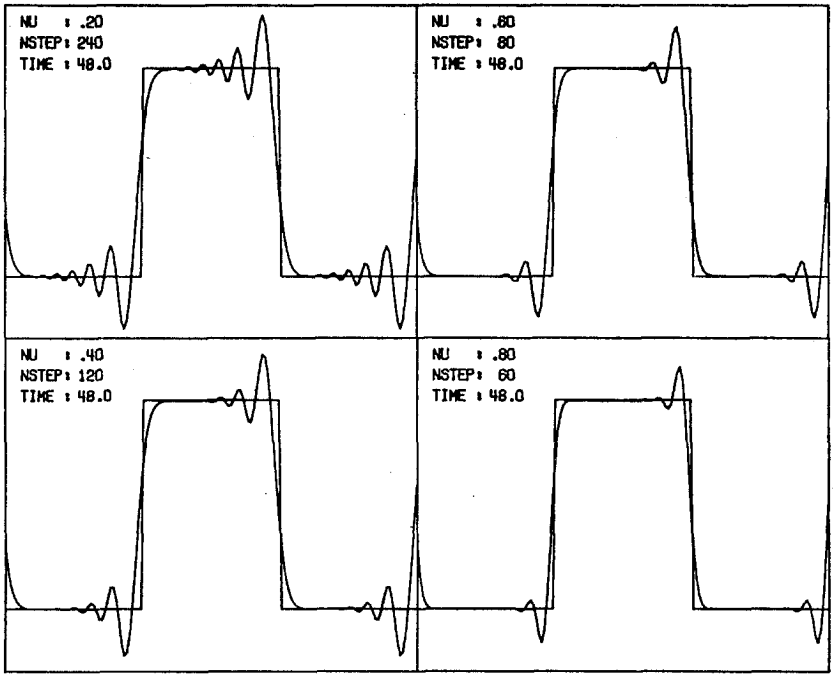

FIG. 4.5. Results for (1.1) with square wave initial data with quadratic interpolation and $\alpha = 0.5$, i.e., the classical Lax–Wendroff scheme. Note the considerable dispersion.

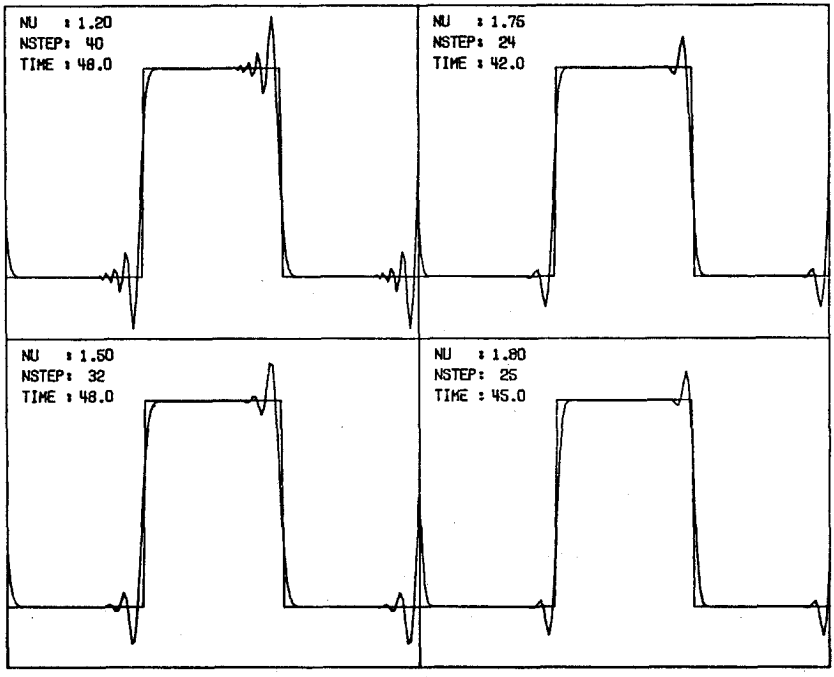

FIG. 4.6. Results for (1.1) with square wave initial data with quadratic interpolation and $\alpha = 1.0$. This scheme exhibits less dispersion than the classical Lax–Wendroff method.

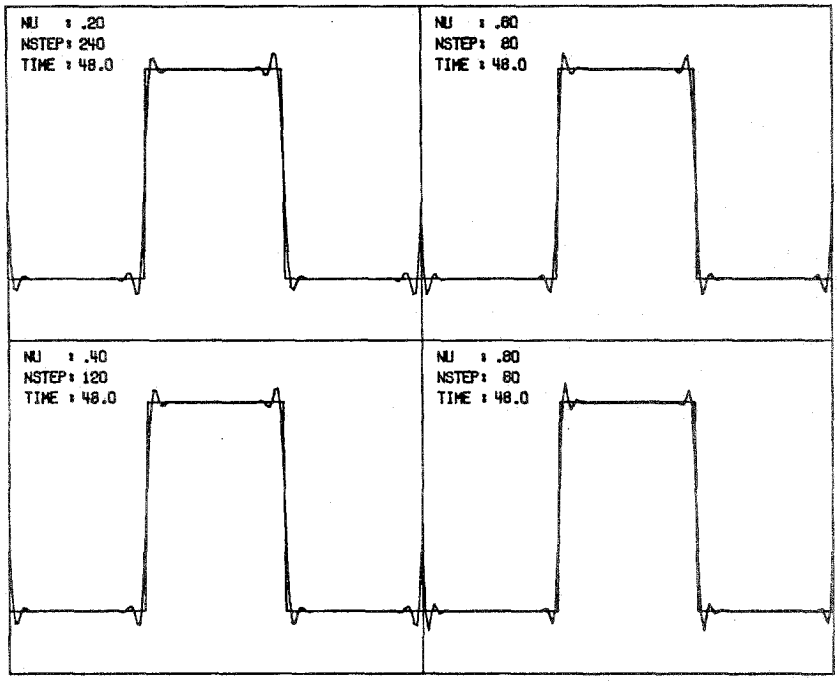

FIG. 4.7. Results for (1.1) with square wave initial data, $\alpha = 0.6$ and quintic interpolation. Clearly there is a considerably less dispersion than with quadratic interpolation.

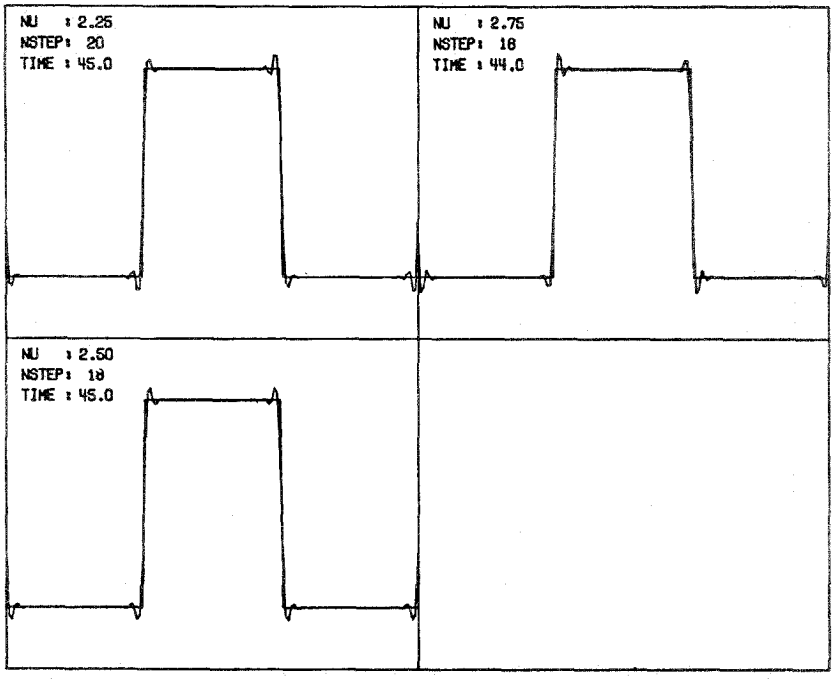

FIG. 4.8. Results for (1.1) with square wave initial data, $\alpha = 1.0$ and quintic interpolation. The dispersion error is smallest with $\alpha = 1.0$.

Courant number ν for various values of α. The curve with $\alpha = 0.5$ in Fig. 4.1 represents results from the classical Lax–Wendroff scheme. Note: ν was varied by setting c and Δx to one and varying Δt. T represents the final time.

In all four figures the errors accumulated in the numerical schemes were due to phase shifts. Note that by varying α we can change the value of ν at which the difference schemes satisfy the shift condition, i.e., the value of ν at which the scheme is exact. And as the order of interpolating polynomial increases, the number of points at which the difference schemes satisfy the shift condition increases. The shift condition is satisfied at points $\nu = k\alpha - i$, where i ranges from 1 to k. Clearly if $\alpha < 1$ the range of i is up to the point where ν becomes negative.

TABLE II

Quintic Interpolation with Square Wave Initial Data

	α			
ν	0.5	0.6	0.8	1.0
0.1	*G*	*G*	*B*	*B*
0.2	*G*	*G*	*B*	*B*
0.4	*G*	*G*	*B*	*B*
0.5	*E*	*G*	*B*	*B*
0.6	*B*	*G*	*B*	*B*
0.8	*B*	*G*	*B*	*B*
1.0	*B*	*E*	*E*	*E*
1.2	*B*	*B*	*G*	*B*
1.4	*B*	*B*	*G*	*B*
1.5	*E*	*B*	*G*	*B*
1.6	*B*	*B*	*G*	*B*
1.8	*B*	*B*	*G*	*B*
2.0	*B*	*E*	*E*	*E*
2.2	*B*	*B*	*B*	*G*
2.4	*B*	*B*	*B*	*G*
2.5	*E*	*B*	*B*	*G*
2.6	Unstable	*B*	*B*	*G*
2.8	↓	*B*	*B*	*G*
3.0		*E*	*E*	*E*
3.2		Unstable	*B*	*B*
		↓	*B*	*B*
3.8			*B*	*B*
4.0			*E*	*E*
4.2			Unstable	*B*
			↓	
4.8				*B*
5.0				*E*
				Unstable
				↓

Note. *E*—exact answer; *G*—result is comparable to Figs. 4.7, 4.8; *B*—severe oscillations present. The trend in the numerical results continues for $\alpha > 1$.

The stability constraints for the individual difference schemes are easily determined with the heuristic stability analysis presented earlier. For example, consider Fig. 4.4 with $\alpha = 1.0$ and recall $c = 1$. Also recall the characteristic equation, along which the solution is propagated, has the form $dt/dx = 1$. We also note that for the triangular element in question $dx = 5\Delta x = 5$ (since $\Delta x = 1$). Thus the characteristic data will not fall within the triangular element and the scheme is unstable. However, if $\Delta t \leqslant 5$ the charactristic data for the solution at the $(n+1)$st time level is included in the triangular element.

In all cases that we have studied (i.e., up to $O(h^5)$) the heuristic stability analysis appears to predict the correct results.

An interesting result that we have been unable to explain is depicted in Fig. 4.4. The values of ν that lie between the arrows for a particular α (e.g., with $\alpha = 0.8$ the region with ♂ ♉, i.e., $3 < \nu < 4$) have errors of $O(10^{-3})$, which are two orders of magnitude larger than predicted. These errors are not caused by phase shift.

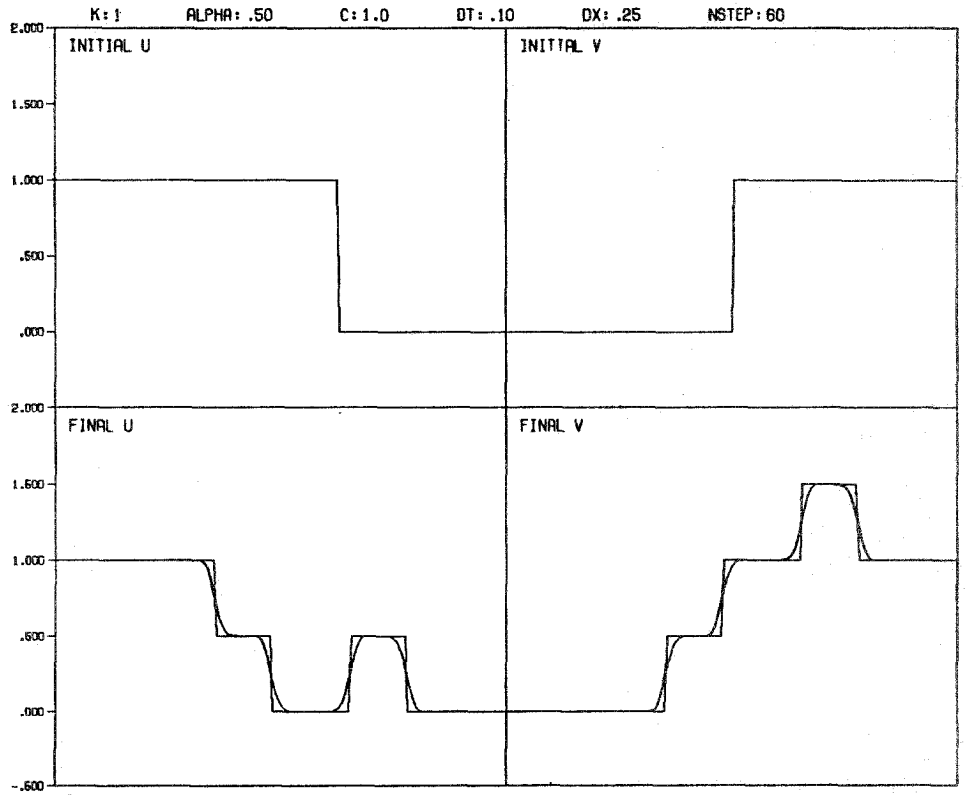

FIG. 4.9. Results for the system (2.2a) with square wave initial data, $\alpha = 0.5$, $\nu = 0.4$, and linear interpolation.

For various values of v and α, Figs. 4.5 and 4.6 represent results for (1.1) with quadratic interpolating polynomials and square wave initial data. In particular Fig. 4.5 represents results for the Lax–Wendroff scheme, i.e., $\alpha = 0.5$.

Figures 4.7 and 4.8 represent results for (1.1) with quintic interpolation and square wave initial data.

In all cases, for interpolating polynomials of second order up to polynomials of fifth order, we found dispersive errors. In general, however, the dispersion decreased with higher order interpolation. The slopes of the numerical solutions at the wave fronts were also much more accurate for higher order polynomials.

Recall k is the order of polynomial interpolation.

A very useful result of the study can be found in Table II. That is, for a fixed α, $v \in (k(\alpha - \frac{1}{2}) - \frac{1}{2}, k(\alpha - \frac{1}{2}) + \frac{1}{2})$ will produce best results. However, by varying α one can cover a very large range of values of v and still maintain good results. (For example, using quintic interpolation we set $\alpha = 0.5$ for $v \leqslant 0.5$, then change to $\alpha = 0.6$ for $0.5 \leqslant v \leqslant 1.0$, then change to $\alpha = 0.8$ for $1.0 \leqslant v \leqslant 2.0$, then change to $\alpha = 1.0$ for

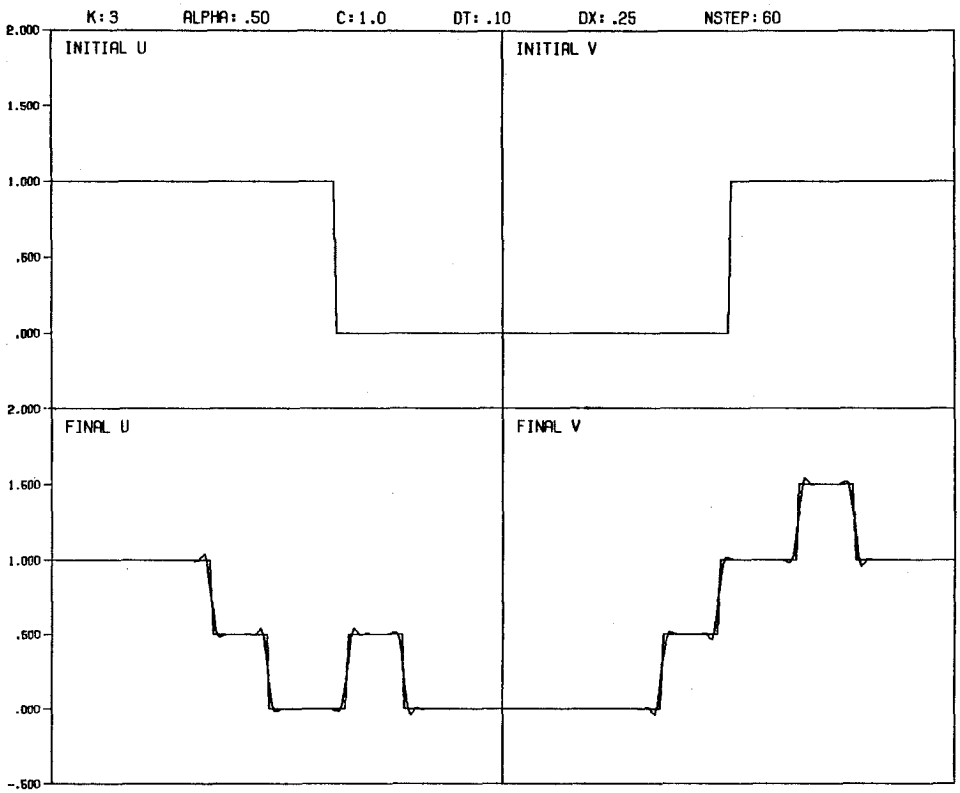

FIG. 4.10. Results for the system (2.2a) with square wave initial data, $\alpha = 0.5$, $v = 0.4$, and cubic interpolation.

$2.0 \leqslant \nu \leqslant 3.0$, etc.) The term "good results" means results comparable to Figs. 4.7 and 4.8. Although Table II only contains results for quintic interpolation the same statement holds true for lower order interpolation.

Figures 4.9–4.11 represent results for the system (2.2a), which corresponds to the second order equation (1.2). In all three figures $\nu = 0.4$, $\alpha = 0.5$ and the numerical results are presented after 60 time steps. The upper half of each figure presents the initial distribution for u and v.

The results for the system are very similar to the results for the single equation (1.1). Figure 4.9 (linear interpolation) is the only figure of the three that has a dominant dissipative error. All of the higher order polynomial interpolation schemes we checked had dominant dispersive errors, e.g., see Figs. 4.10 (cubic interpolation) and 4.11 (quintic interpolation).

The same basic conclusion previously drawn from numerical results for (1.1) hold for (2.2a). However, due to the introduction of two characteristic equations, the C.F.L. stability criteria for (2.2a) is stricter and there is less freedom to vary α.

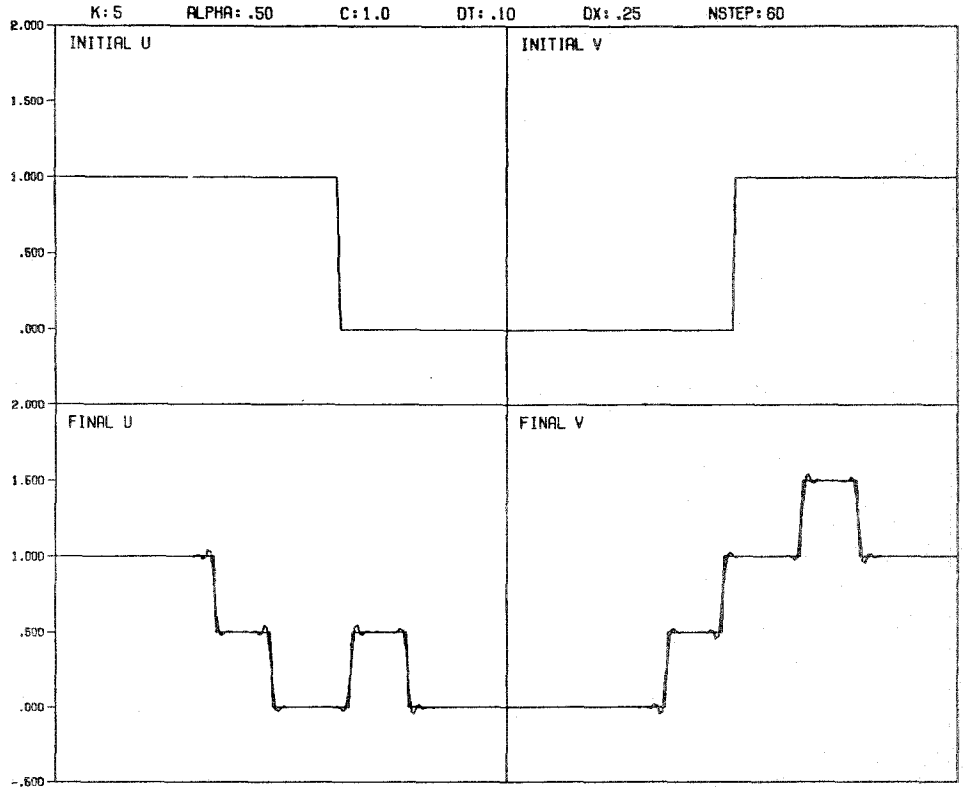

FIG. 4.11. Results for the system (2.2a) with square wave initial data, $\alpha = 0.5$, $\nu = 0.4$, and quintic interpolation.

5. Nonlinear Example

In the previous section we examined the use of our method on linear equations. At this point we would like to present a nonlinear example.

Consider the shallow water (compressible gas) equations in the following form:

$$\begin{pmatrix} u \\ v \end{pmatrix}_t + \begin{pmatrix} u & 2v \\ \frac{1}{2}v & u \end{pmatrix}\begin{pmatrix} u \\ v \end{pmatrix}_x = \begin{pmatrix} 0 \\ 0 \end{pmatrix}, \qquad \begin{pmatrix} u(x,0) \\ v(x,0) \end{pmatrix} = \begin{pmatrix} f(x) \\ h(x) \end{pmatrix}. \tag{5.1}$$

With our numerical technique (5.1) may be solved in two ways. The first technique, which is quite inefficient, would be to expand the entire system in terms of Lagrange polynomials. This would lead to a system of nonlinear algebraic equations which must be solved at each node. The second method (the method we choose to use) is more efficient. In this case the square matrix in (5.1) is considered constant over each element. This method then produces a system of linear algebraic equations that must be solved at each node.

Figures 5.1 through 5.3 represent numerical results for (5.1) with initial data

$$\begin{aligned} f(x) &= 0, & x &\geqslant 0, \\ h(x) &= 20, & x &\geqslant 0, \\ v(0,t) &= 20 + t, & t &\geqslant 0. \end{aligned} \tag{5.2}$$

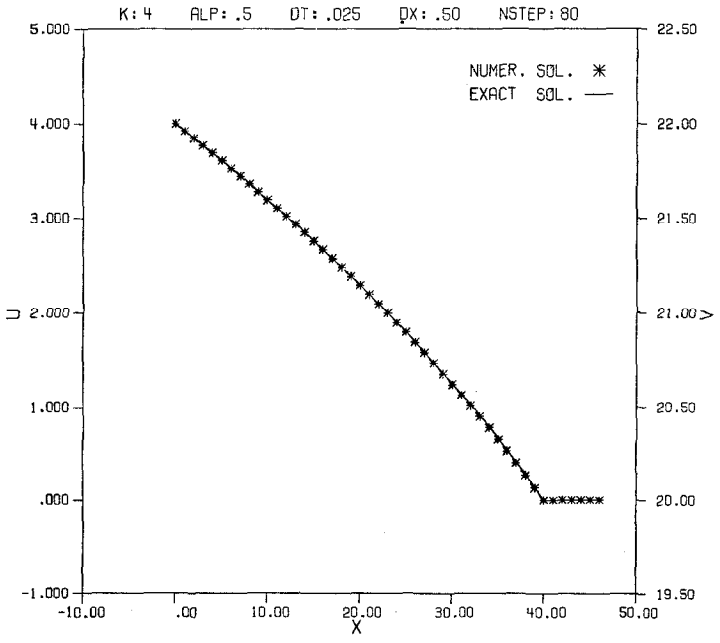

FIG. 5.1. Comparison of numerical and analytical results for the shallow water equations using quartic interpolation.

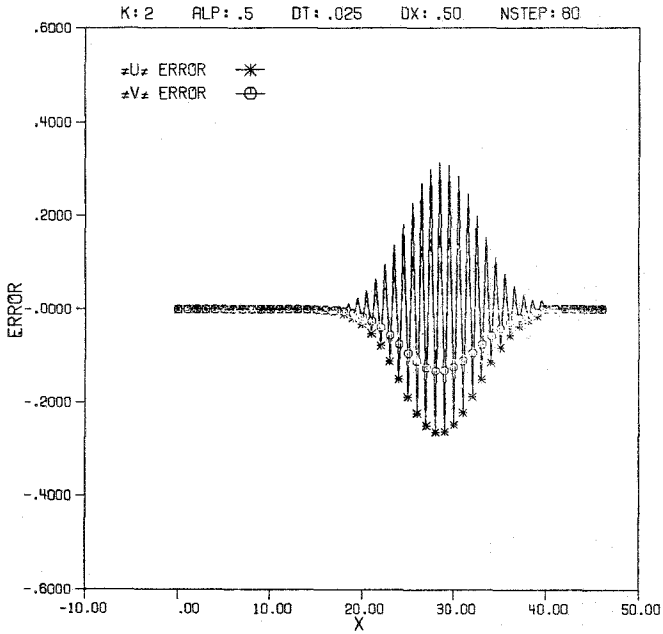

FIG. 5.2. Error plot for the numerical solution to the shallow water equations with quadratic interpolation.

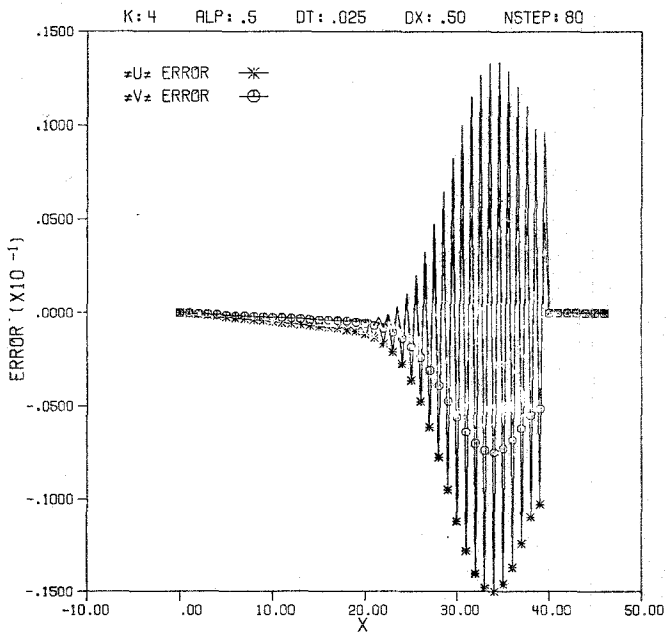

FIG. 5.3. Error plot as in Fig. 5.2 with quartic interpolation.

Figure 5.1 is a plot of the analytical solution of (5.1) subject to (5.2) versus our numerical solution at time $t = 2$. In this case quartic interpolation was used with $\alpha = \frac{1}{2}$ and the square matrix evaluated at one node left of center at time level n in each element. As can be seen the results are quite good.

Figures 5.2 and 5.3 are plots, for $\alpha = \frac{1}{2}$, of the error induced by using quadratic and quartic polynomials, respectively. Note the considerable improvement derived by using higher order interpolation.

As in quartic case, when quadratic interpolation was used the square matrix in (5.1) was evaluated at one node left of center at time level n (upstream weighting).

The stability analysis for the nonlinear equation is analogous to that in Section 3 only v now involves the eigenvalues of the square matrix in (5.1). Note that v varies from element to element.

6. Conclusions

The major contribution of this work is that we have presented a technique for generating explicit, arbitrary high order accuracy schemes for linear wave-type equations. The numerical results presented involved the solution of two very simple linear equations, and a more complex nonlinear problem. The technique, however, is applicable to other wave-type equations possessing a backward light cone data set.

It is interesting to note that by varying the parameter α (the shape of the triangular element) we may generate a continuous spectrum of difference schemes. The stability of the schemes depends on both α and v, and for (1.1) by choosing the appropriate value of α any v can be used. Also, for (1.1) the schemes are stable for $k(\alpha - 1) \leqslant v \leqslant k\alpha$.

Another important fact brought out in the numerical results section is that by varying α for (1.1), we considerably increase the range of v over which a given order of polynomial interpolation produces good results, i.e., by increasing α periodically the stability criteria also increases. Standard finite difference schemes do not possess this property.

For every order of polynomial interpolation we examined (greater than first and up to $O(h^5)$) we found dispersive errors. However, these errors decreased with increasing order of interpolation.

The computational implementation of the procedure is quite simple. A change in the order of accuracy of the method requires only a slight programming change. Similarly (though varying α may considerably improve the numerical results over a given range of v) variations in α can be handled with no programming changes. Computationally, the inversion of A is the only time consuming process.

One final point that should be brought out is that free boundary problems and problems with rapidly varying gradients can be handled in an easy fashion with the technique presented. This follows from the ease in varying α and hence the nodal spacing.

We should at this point mention some important drawbacks to the methods presented in this article.

The major drawback of the method in its present form pertains to nonlinear equations (e.g., (5.1)). The difficulty encountered is that the matrix A in (2.3d) must be inverted at each node owing to the nonlinear equation. For orders of interpolation less than four this problem however can be overcome by linearizing (as is typically done with difference schemes) and inverting the linear system analytically (see, for example, (A.2) of the Appendix). For higher orders of interpolation it is difficult to analytically invert the matrix A.

An effort is currently being put forth to find a general inverse to A of (2.3d) for arbitrary orders of interpolation.

It is important to note that at the sacrifice of efficiency fully nonlinear systems can be solved. One must decide for himself how much efficiency he is willing to give up for higher numerical precision.

We believe the overall methods have great promise. If and when one is able to write out an analytically explicit equation for the difference formulas of higher order a considerable amount of the difficulties encountered with nonlinear equations should be overcome.

APPENDIX

Using the notation of Fig. A.1 with linear interpolating polynomials, and applying Galerkin's method over a single element (e) we find (Cushman [2])

$$u^{n+\beta}_{j+(2\alpha-1)\gamma} = \left(\frac{\beta}{2\gamma}\nu - \alpha + 1\right) u^n_{j-\gamma} + \left(\alpha - \frac{\beta}{2\gamma}\nu\right) u^n_{j+\gamma}. \tag{A.1}$$

The Euler, Lax, and upstream differencing schemes can be derived respectively by setting:

(i) $\alpha = 0, \gamma = \frac{1}{2}, \beta = 1,$

(ii) $\alpha = \frac{1}{2}, \gamma = 1, \beta = 1,$ and

(iii) $\alpha = 1, \gamma = \frac{1}{2}, \beta = 1.$

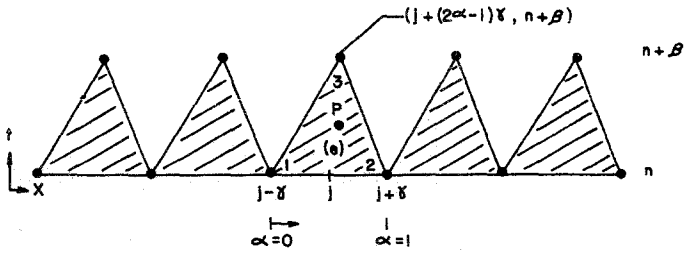

FIG. A.1. Representation of the elements for linear interpolation, first order, single-step, explicit methods.

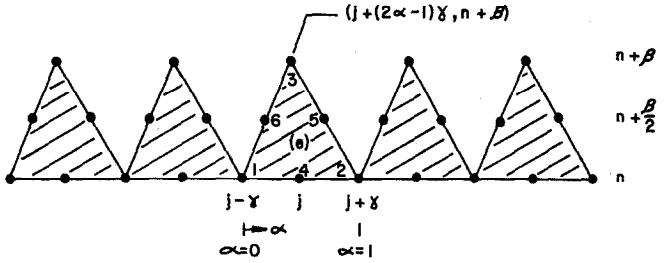

FIG. A.2. Representation of the elements for quadratic interpolation, second order, single-step, explicit methods.

Figure A.2 illustrates the location of the various nodel points for quadratic interpolation. If we again apply Galerkin's method, only now use quadratic interpolation polynomials and test functions, we derive:

$$A\bar{x} = B\bar{y}, \tag{A.2}$$

where

$$A = \begin{bmatrix} (-8\beta\nu + 16\alpha\gamma - 16\gamma) & -6\gamma & (8\beta\nu - 16\alpha\gamma + 8\gamma) \\ (-2\beta\nu + 4\alpha\gamma + 2\gamma) & -4\gamma & (2\beta\nu - 4\alpha\gamma + 6\gamma) \\ (-8\beta\nu + 16\alpha\gamma - 8\gamma) & -6\gamma & (8\beta\nu - 16\alpha\gamma) \end{bmatrix},$$

$$B = \begin{bmatrix} (\beta\nu - 2\alpha\gamma + 2\gamma) & (-4\beta\nu + 8\alpha\gamma - 16\gamma) & (3\beta\nu - 6\alpha\gamma) \\ (\beta\nu - 2\alpha\gamma + 2\gamma) & 2\gamma & (-\beta\nu + 2\alpha\gamma) \\ (-3\beta\nu + 6\alpha\gamma - 6\gamma) & (4\beta\nu - 8\alpha\gamma - 8\gamma) & (-\beta\nu + 2\alpha\gamma) \end{bmatrix},$$

$$\bar{x} = \begin{bmatrix} u^{n+\beta/2}_{j+\alpha\gamma} \\ u^{n+\beta}_{j+(2\alpha-1)\gamma} \\ u^{n+\beta/2}_{j+(\alpha-1)\gamma} \end{bmatrix}, \quad \text{and} \quad \bar{y} = \begin{bmatrix} u^{n}_{j-\gamma} \\ u^{n}_{j} \\ u^{n}_{j+\gamma} \end{bmatrix}.$$

As a special case if we set $\alpha = \frac{1}{2}$, $\gamma = 1$, and $\beta = 1$, invert A and solve for u^{n+1}_j we derive the single-step $O(\Delta t^2, \Delta x^2)$ Lax–Wendroff scheme.

REFERENCES

1. J. H. CUSHMAN, Difference schemes or element schemes, *Int. J. Num. Meth. Eng.* **14** (1979), 1643–1651.
2. J. H. CUSHMAN, An elementary relationship between finite difference and finite element equations, submitted for publication.
3. C. A. FELIPPA, "Refined Finite Element Analysis of Linear and Nonlinear Two-Dimensional Structures," Rep. SESM 66–22, Stuctural Eng. Lab., University of California, Berkeley, 1966.
4. R. H. GALLAGHER AND S. T. K. CHAN, Higher-order finite element analysis of lake circulation, *Comput. Fluids* **1** (1973), 119–132.

5. J. T. ODEN AND J. N. REDDY, "An Introduction to the Mathematical Theory of Finite Elements," Wiley–Interscience, New York, 1976.
6. P. J. ROACHE, "Computational Fluid Dynamics," Hermosa, Albuquerque, 1972.
7. V. V. RUSANOV, On differences schemes of third-order accuracy for nonlinear hyperbolic systems, *J. Comp. Phys.* **5** (1970), 507–516.
8. A. H. STROUD, Integration formulas for the wave equation in n-space dimensions. *J. Comp. Phys.* 25 (1977), 32–55.
9. R. F. WARMING, P. KUTLER, AND LOMAX, Second- and third-order noncentered difference schemes for nonlinear hyperbolic equations. *AIAA J.* **11** (1973), 189–196.
10. H. F. WEINBERGER, "A First Course in Partial Differential Equations," Blaisdell, Waltham, Mass., 1965.
11. A. WOUK, "A Course of Applied Functional Analysis," Wiley–Interscience, New York, 1979.